QUARK DISTRIBUTIONS IN NUCLEI AND DEEP INELASTIC SCATTERING OF CHARGED LEPTONS

K. Rith
Fakultät für Physik
Universität Freiburg
Hermann-Herder-Str. 3
D-7800 Freiburg i. Br.

1. INTRODUCTION

Deep inelastic lepton (electron, muon, neutrino) scattering experiments are the basic tool to study the internal structure of hadronic matter. The results of these experiments have established our understanding of nucleons as a collection of quarks and gluons and have provided us with a lot of information about the momentum distribution of these constituents inside the nucleon and in general about their interactions as described by Quantum Chromodynamics (QCD). Recently the European Muon Collaboration (EMC) has discovered in a muon scattering experiment off deuterium and iron targets that these distributions are different for nucleons, which are embedded in nuclei, and for free nucleons {1}. These results caused a lot of excitement and they may help a lot for the understanding of nuclear physics in terms of quarks and gluons, which is the general topic of this conference. In this contribution I will briefly recall the phenomenology of deep inelastic scattering experiments, discuss the experimental data and their consequences and review the theoretical models which are available at present.

2. PHENOMENOLOGY OF DEEP INELASTIC SCATTERING OF CHARGED LEPTONS

In a deep inelastic scattering process the charged lepton ℓ (electron, muon) interacts with a nucleon via the exchange of a virtual photon γ or a neutral vector boson Z_o. (In the following discussion I will neglect the Z_o, because at present accelerator energies its contribution to the cross section is very small {2}). In the Quark Parton Model {3} the virtual photon couples to the charge of one of the pointlike, quasifree quarks which might be either one of the valence quarks (u_v, d_v) or a member of the quark-antiquark pairs contained in the 'sea'(u_s, $\bar{u}_s$, d_s, $\bar{d}_s$, s_s, $\bar{s}_s$, c_s, $\bar{c}_s$, ...). The process is shown in fig. 1.

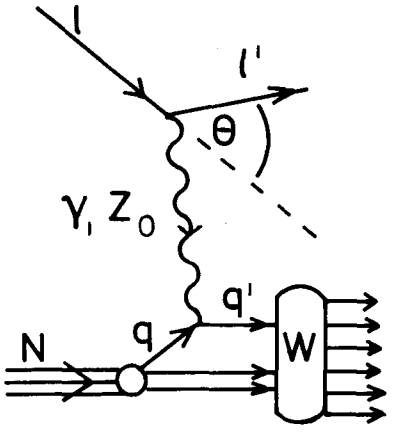

Fig. 1. Quark-Parton-Model picture of deep inelastic charged lepton nucleon scattering.

The two quantities which controll the interaction are Q^2 and x. Q^2 is the negative square of the fourmomentum carried by the virtual photon and is in the laboratory system given by $Q^2 = 2EE'(1-\cos\theta)$, E and E' being the energies of incoming and outgoing lepton and θ the lepton scattering angle. Q^2 is a measure of the spatial resolution $\lambda \sim 1/\sqrt{Q^2}$ at which the nucleon is probed. Present muon experiments reach values of Q^2 around 200 GeV^2 which correspond to a resolution of about 10^{-15}cm. The quantity x is defined as $x = Q^2/2M\nu$, where M is the nucleon mass and $\nu = E-E'$ is the energy transferred by the virtual photon from the lepton to the hadronic final state of mass W. In an infinite momentum frame {4} x can be interpreted as the fraction of the nucleon momentum carried by the interacting quark. It can be selected by a suitable choice of Q^2 and ν or E, E' and θ, respectively.

In the one photon exchange approximation the double differential cross section in terms of these two quantities can be written, using $y = \nu/E$, as

$$\frac{d^2\sigma}{dQ^2dx} = \frac{4\pi\alpha^2}{Q^4} \left\{ \left(1-y-\frac{Mxy}{2E}\right) \frac{F_2(x,Q^2)}{x} + F_1(x,Q^2)y^2 \right\} \qquad (1)$$

Apart from kinematical factors this cross section depends on a combination of two structure functions $F_1(x,Q^2)$ and $F_2(x,Q^2)$. These two structure functions contain informations about the charge and spin of the quarks similar to the electromagnetic form factors in the case of elastic electron-nucleon and electron-nucleus scattering. The form factors can be related to the Fourier transforms of the spatial distribution of charge and magnetic moment of the nucleon or nucleus and show a strong Q^2 dependence because these are extended objects. In the case of scattering off point-like particles the Fourier transform is a constant and therefore no Q^2 dependence of the structure functions should be observed, what in first approximation is indeed

the case.

F_1 and F_2 are linked by the ratio $R = \sigma_\ell/\sigma_t$ of the longitudinal to transverse virtual photon cross section via the expression

$$2 \times F_1 = F_2 \, (1 + Q^2/\nu^2)/(1 + R). \qquad (2)$$

For spin - $\frac{1}{2}$ constituents $\sigma_\ell = 0$ and $R = 0$ and consequently

$$2 \times F_1 \approx F_2 \, ,$$

while for spin 1 constituents $\sigma_t = 0$, $R = \infty$ and $F_1 = 0$. Experimental results show {5} that at high Q^2 R is approximately equal to zero: quarks indeed carry spin $\frac{1}{2}$. The structure function F_2 is related to the quark charges and is given by

$$F_2(x) = \sum_f Q_f^2 \, x \, (q_f(x) + \bar{q}_f(x)), \qquad (3)$$

where the sum runs over the different quark flavours, Q_f is the charge number of the quarks and $q_f(x)$ $(\bar{q}_f(x))$ is the probability that a quark (antiquark) of flavour f carries the fraction x of the nucleon momentum. The quantities $q_f(x)$ are also called quark distribution functions.

Let us apply this expression to the cases where the scattering takes place off a deuterium or a iron target.

If there are no binding effects, the structure function F_2^N per nucleon for the deuteron is given by the sum of the structure functions for a free proton and a free neutron

$$F_2^N(D) = \frac{1}{2} (F_2^p + F_2^n)$$

$$= \frac{5}{18} \, x \, \{u(x) + \bar{u}(x) + d(x) + \bar{d}(x) + s(x) + \bar{s}(x) + c(x) + \bar{c}(x)\}$$

$$- \frac{1}{6} \, x \, \{c(x) + \bar{c}(x) - s(x) - \bar{s}(x)\} \qquad (4)$$

The distributions u(x) and d(x) contain contributions from valence and sea quarks:

$u(x) = u_v(x) + u_s(x)$, $d(x) = d_v(x) + d_s(x)$, while the other distributions correspond to seaquarks only.

If there are no nuclear effects the structure functions F_2^N per nucleon for iron is given by

$$F_2^N(\text{Fe}) = \frac{1}{56}(30\,F_2^n + 26\,F_2^p) = F_2^N(\text{D})\,(1-K(x)), \tag{5}$$

with

$$K(x) = \frac{1}{14}\,\frac{F_2^p - F_2^n}{F_2^p + F_2^n} \tag{6}$$

K(x) is a correction factor which takes into account that iron is no isoscalar target and that proton and neutron structure functions are different. Approximating F_2^n by {6}:

$$F_2^n \approx (1-0.75x)\,F_2^p\,,$$

one gets for x = 0.65, the highest x-value covered by the EMC data, a correction of $\sim$ 2.3%.

The x dependence of the structure function F_2 and of the contributions coming from the valence quarks and from the sea quarks is shown in fig. 2.

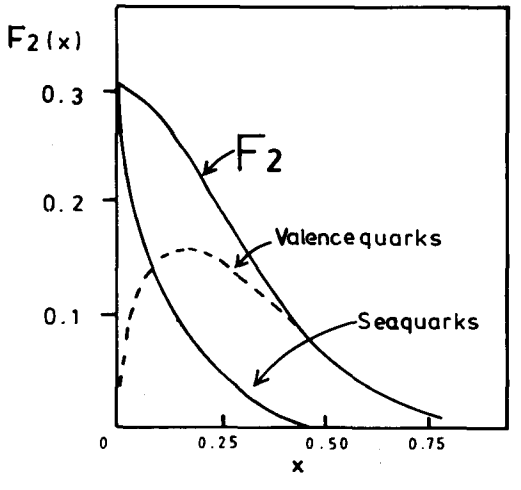

Fig. 2. The nucleon structure function F_2.

It must be mentioned here that the separation in valence and sea part can not be done in a direct way with electron or muon scattering experiments alone, for the virtual photon just couples to the charge of the quarks independent of their flavour. This is different in the case of neutrino scattering. Neutrinos and antineutrinos couple differently to different flavours and to quarks and antiquarks and the sea quark distribution can be extracted by a combination of antineutrino and neutrino cross sections {7}.

As can be seen from this figure sea quarks dominate at low x but their contribution has disappeared at values of x around 0.4 - 0.5.

Gluons do not contribute directly to the cross section obtained in deep inelastic scattering. But they show up indirectly. If one sums over all momentum fractions x and all probabilities q(x), this sum should yield 1 and the momentum integral $\int_0^1 F_2^N \, dx$ of equation (4) should give $\frac{5}{18}$. Experimentally this integral is only around 45% of the expected value, which shows that only 45% of the nucleon momentum is carried by charged quarks, the remaining 55% must be carried by neutral constituents, the gluons. Therefore the momentum sum rule has to be modified to

$$\int_0^1 (F_2^N + x\, g(x))\, dx = \frac{5}{18} \qquad (7)$$

g(x) is the momentum distribution of the gluons inside the nucleon.
g(x) and q(x) are correlated by the elementary QCD processes of gluon emission by quarks and the creation of quark-antiquark pairs out of gluons.

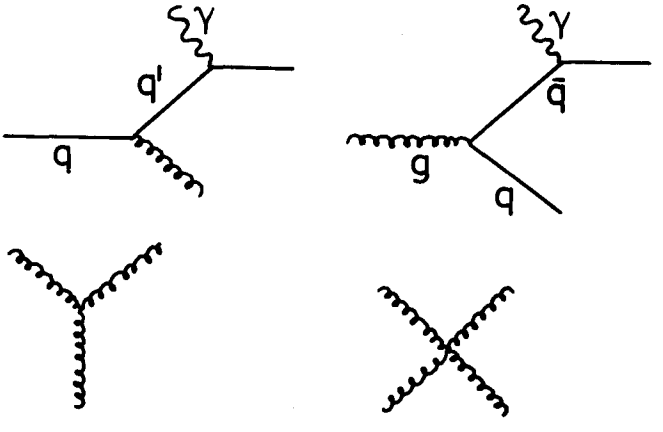

Fig. 3. First order QCD processes

Due to these processes and gluon-gluon interactions shown in fig. 3 the momentum distributions and the structure functions become Q^2-dependent: they are depleted with increasing Q^2 at high x and enhanced at low x as shown in fig. 4a as a function of x for different Q^2 and in fig. 4b as a function of Q^2 for fixed values of x.

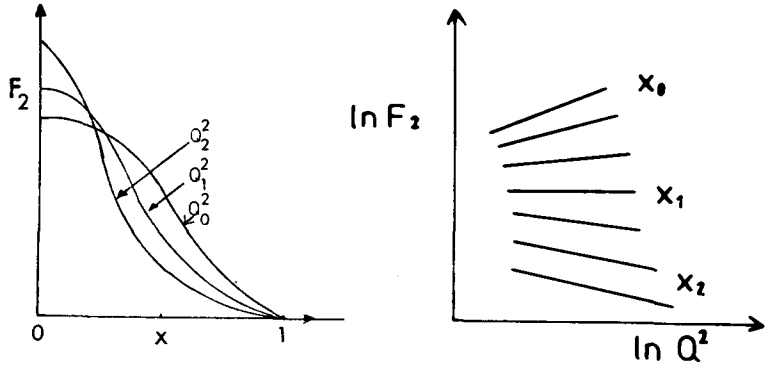

Fig. 4. The x-Q^2 dependence of F_2 due to QCD processes.
a) for fixed Q^2 ($Q_o^2<Q_1^2<Q_2^2$), b) for fixed x ($x_o<x_1<x_2$)

The coupling of $g(x)$ and $q(x)$ and their logarithmic Q^2-dependence is expressed by the Altarelli-Parisi-equations {8}. Thus the analysis of the pattern of scale breaking of the structure functions with Q^2, as shown in fig. 4b, in terms of these equations allows a determination of the gluon distribution $g(x)$ and its Q^2-dependence {9}.

Up to now we have only discussed the case of free nucleons and we have assumed that, apart from simple kinematical effects due to the Fermi motion of the nucleons, the quark and gluon distributions are not altered due to the neighbouring nucleons inside the nucleus. This might be a good approximation for the deuteron which is only a loosely bound system with a mean center to center nucleon distance of about 4 fm compared to the mean nucleon charge radius of $\sim$ 0.8 fm. But already in medium-weight nuclei the nucleons are packed much tighter together. Therefore there might be a lot of nuclear effects which can change the quark and gluon distributions compared to the free nucleon case.

3. THE EXPERIMENTAL DATA

Indeed nuclear effects in deep inelastic muon scattering at high Q^2 have been observed by the EMC by comparing structure functions for iron and deuterium. This group has measured the structure functions for hydrogen {10}, deuterium {11} and iron {12}. Apart from the different targets the identical apparatus has been used for these measurements and the data have been treated with the same analysis chain. Therefore a comparison can be made where the systematic errors are well understood. The apparatus is shown in fig. 5. It is fully described elsewhere {13}.

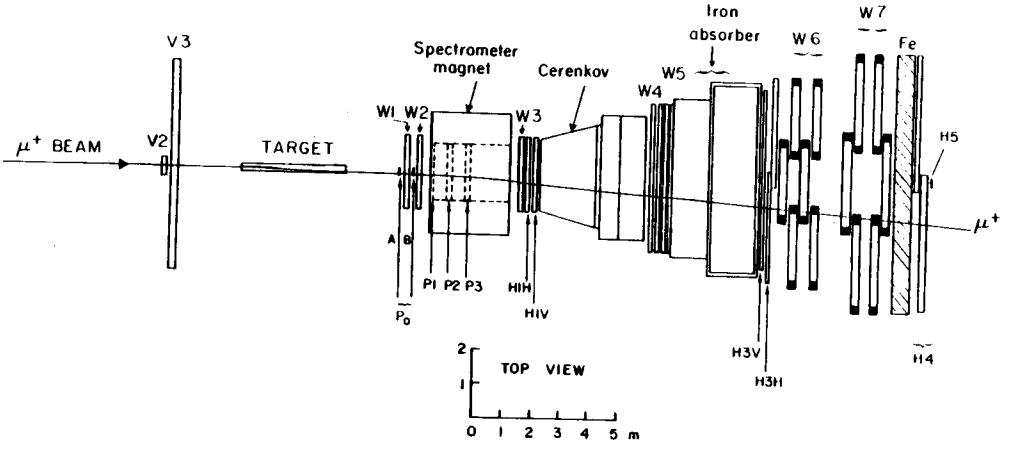

Fig. 5. The EMC Forward Spectrometer

The muon beam was incident either on a 6 m long target of liquid hydrogen or deuterium or on an iron scintillator target. Momentum and direction of the incoming muons were determined in a set of scintillator hodoscopes with high time and space resolution. Scattered muons were detected and momentum analyzed by a system of drift-and multi-wire-proportional-chambers W1 - W5, P1 - P3 and a large aperture (1 x 2 x 4 m^3) air gap dipole magnet and recorded in drift chambers W6, W7 after they had penetrated through a lead-iron-scintillator calorimeter and a 2 m thick iron hadron absorber.

The iron data have been obtained at four muon beam energies of 120, 200, 250 and 280 GeV and contain altogether one million events. The values of the nucleon structure function F_2^N (Fe) = $\frac{1}{56} F_2^{\mu Fe}$ are shown in fig. 6a as a function of Q^2 for fixed values of x. The data are corrected for the nonisoscalarity of iron according to equation (6) so that they correspond to a hypothetical target with the same number of protons and neutrons, no Fermi-motion corrections have been applied. The errors shown are statistical only. Apart from statistical fluctuations there is perfect agreement between these four data sets and the x and Q^2 dependence is very well defined. The rise with Q^2 at low x and the fall with Q^2 at high x, as predicted by QCD, shows up nicely. The solid lines represent a simple parametrization of the iron data, the dashed lines indicate where one would expect the deuterium data relative to the iron data according to Fermi motion model predictions a la Bodek and Ritchie {14}. Predictions of several nuclear Fermi motion models are shown in fig. 7 where the ratio of the structure function F_2^A for a nucleus, with mass number A, to the sum of the free nucleon structure functions for proton and neutron, weighted with the corresponding nucleon numbers, is plotted as a function of x for a iron nucleus. For the deuteron these corrections are expected to be much

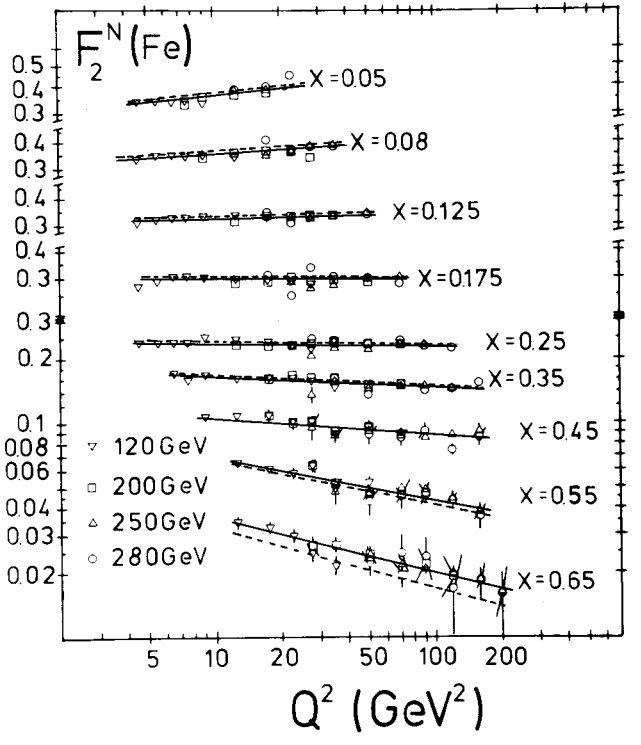

Fig. 6a. The nucleon structure function F_2^N(Fe) for iron as measured by the EMC.

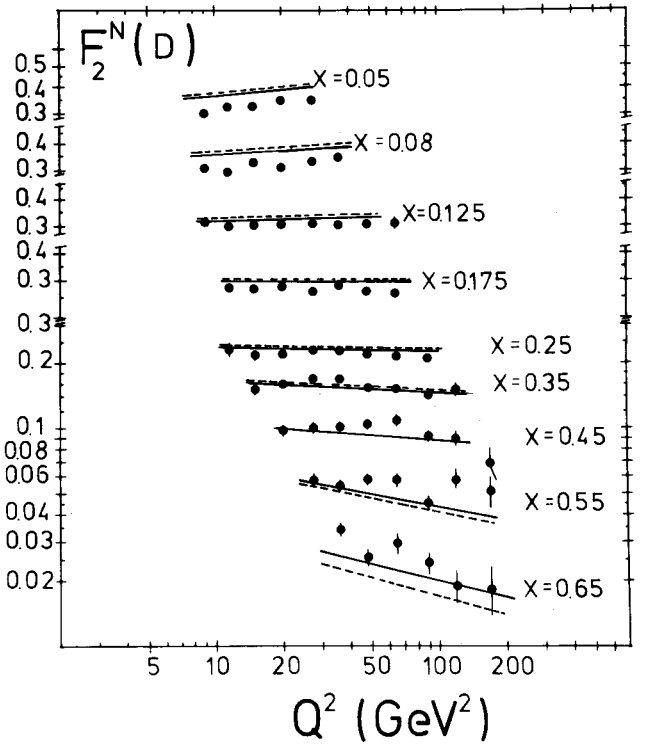

Fig. 6b. The nucleon structure function F_2^N(D) for deuterium as measured by the EMC (muon beam energy 230 GeV)

smaller as can be seen by a comparison with the curve labeled D which shows the deuterium corrections according to Bodek and Ritchie. For discussion of the different Fermi motion models {15} see reference {16}.

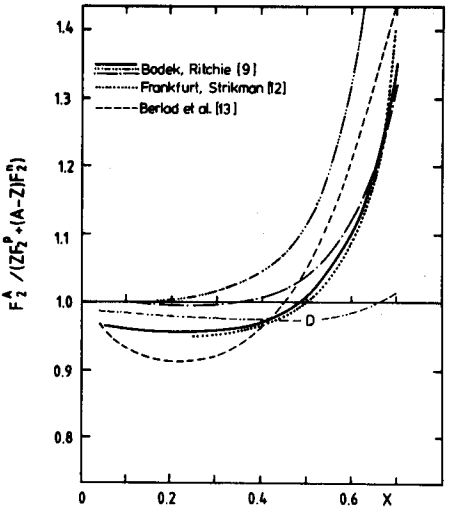

Fig. 7. Fermi motion model calculations for the ratio of the nucleon structure function F_2^A for iron and the weighted sum of the structure functions for proton and neutron.

Deuterium data have been obtained with three muon beam energies of 120, 200 and 280 GeV. The values of $F_2^N(D) = \frac{1}{2} F_2^{\mu D}$, not corrected for Fermi motion, are shown in fig. 6b for the data set taken at 280 GeV. There are negligible changes if the preliminary 200 GeV data are included, the 120 GeV data are still being analyzed. The curves are the same as in fig. 6a, which means that the deuterium data should well be represented by the dashed line if the simple kinematical Fermi-motion models would be correct which assume that the nucleus is a dilute gas of slowly moving nucleons. Obviously this is not the case. At low x the structure function for the iron should be 2-3% smaller than for deuterium but it is larger by about 15%, at high x the iron data should be larger than the deuterium data by about 20-25%, but they are smaller by about 15%. This means that at x around 0.65 there is a discrepancy of 35-40% between Fermi motion model predictions and experimental data. Within the limits of statistical and systematic errors there is no or little Q^2 dependence of this behaviour within the region of overlap of the datasets, which varies from $9 \leq Q^2 \leq 27$ GeV^2 for x = 0.05 over $11.5 \leq Q^2 \leq 90$ GeV^2 for x = 0.25 up to $36 \leq Q^2 \leq 170$ GeV^2 for x = 0.65.

The ratio of the measured nucleon structure functions $F_2^N(Fe)/F_2^N(D)$ has been calculated point by point and then averaged over Q^2 for each value of x. The x dependence is shown in fig. 8 where the error bars are statistical only. The ratio is falling from around 1.15 at x = 0.05 to a value around 0.89 at x = 0.65. A fit of the form

$$F_2^N(Fe)/F_2^N(D) = a + bx \qquad (8)$$

yields a = 1.18 ± 0.01, and for the slope

b = - 0.52 ± 0.04 (stat) ± 0.21 (syst).

A conservative estimate of the possible effect of the systematic uncertainties on the slope is indicated by the shaded area in figure 8.

In terms of quark distributions this result means that a high x (valence quark region) a depletion of the quark momentum distribution in iron comparent to the momentum distribution in a free nucleon is observed, opposite to Fermi motion model predictions, while at low x (sea quark region) where only little difference is predicted, there is an increase.
After the EMC result became known, the SLAC-MIT-Rochester group has realized that the target walls used in SLAC electron-proton and electron deuterium experiments E49 and E87 {17} were constructed from aluminium and steel respectively. The target-wall contributions were measured using empty target replicas, subtracted from the full target rates and then forgotten. These data have been recovered and reanalyzed. The resulting ratios of the cross sections for aluminium to deuterium and steel to deuterium are shown in figures 9a and 9b {18,19}. They span a range of Q^2. The mean Q^2 for the steel data varies from 6.0 GeV^2 (x=0.25) to 19.3 GeV^2 (x=0.9) and for the aluminium data from 1.9 GeV^2 (x=0.075) over 5.2 GeV^2 (x=0.40) to 20.1 GeV^2 (x=0.863). The systematic errors for these data are calculated to be ± 2.3%. Also shown in figure 9b is the EMC result at larger values of Q^2. In the region of overlap the agreement between the two experiments is excellent. A straight line fit to the SLAC data in the region $0.2 \leq x \leq 0.6$ yields a=1.15 ± 0.04 ± 0.011 and b = -0.45 ± 0.05, values which are very similar to the EMC result. The SLAC data extend to higher values of x where the cross section ratio is rising again, indicating that the effects of Fermi motion become dominant there. Also plotted in this figure is the ratio for copper and deuterium from a low Q^2 experiment at SLAC {20} and photoproduction results {21}, which show that at low Q^2 the ratio is considerably reduced due to shadowing effects.
The aluminium results, which are shown in figure 9a together with data from a lower Q^2 experiment at SLAC and photoproduction show a similar trend as that observed for steel, the effect being somewhat weaker. The results for a straight line fit yield

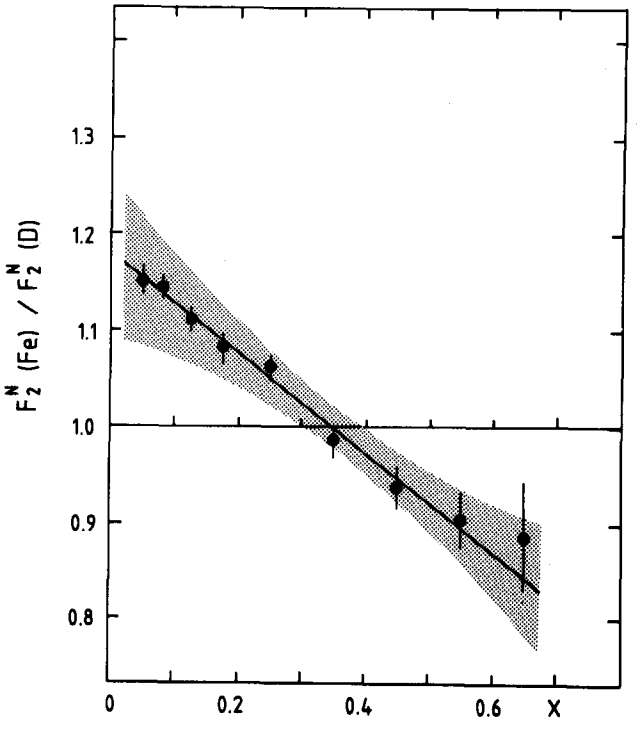

Fig. 3. The ratio of the nucleon structure function F_2^N for iron and deuterium measured by the EMC

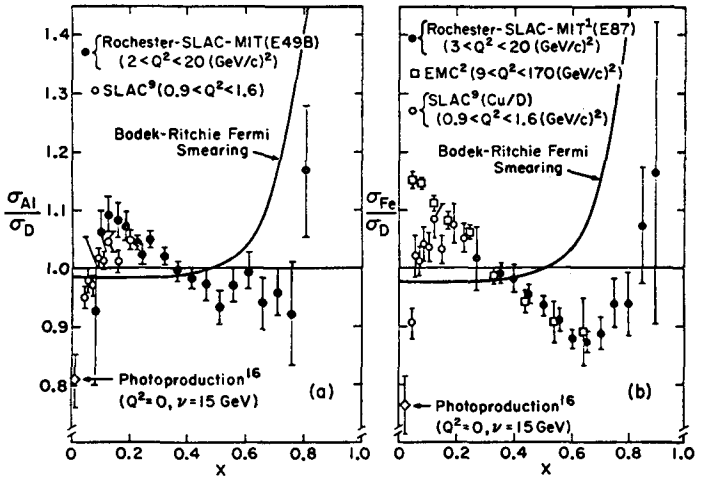

Fig. 9a. σ_{Al}/σ_D measured by SLAC

Fig. 9b. σ_{Fe}/σ_D measured by SLAC

a = 1.11 ± 0.02 ± 0.23 and b = -0.30 ± 0.06, the slope being 1.5 standard deviations lower than for steel.

3. CONSEQUENCES

Taking all this informations together the following picture emerges, which is summarized in figure 10: quark distributions measured in deep inelastic scattering off nuclei $q_A(x)$ are far from being identical with those in free nucleons $q_{n,p}(x)$. In the low x region up to x around 0.25-0.3, where sea quarks are important, nuclear effects cause a significant enhancement of $q_A(x)$ compared to the free nucleon case if Q^2 is large enough ($Q^2 \geq 10$ GeV^2?).

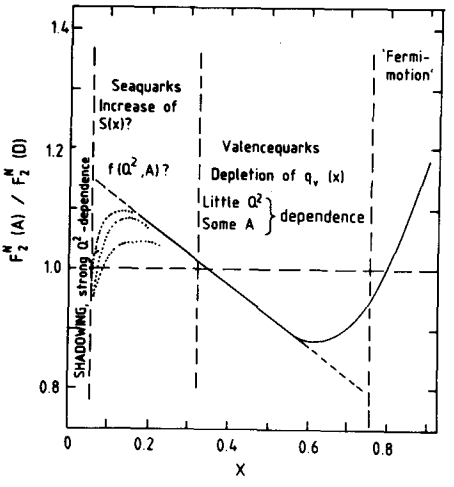

Fig. 10. Possible behaviour of nuclear effects in deep inelastic scattering.

At very low x values, which at present accelerator energies are only accessible at very low Q^2 and by photoproduction ($x=Q^2=0$), A dependent shadowing effects may play the dominant role. The combined effects of nuclear enhancement at low x and shadowing at low Q^2, which are due to completely different physics, may cause a strong Q^2 and A dependence of the observed effect. At medium x ($0.3 \leq x \leq 0.7$), the valence quark region, $q_A(x)$ is depleted opposite to what is expected from Fermi motion effects. The data indicate no or little Q^2 dependence of the effect for $Q^2 > 6$ GeV^2 while probably it is weakly increasing with mass number A. Finally, at even higher x(>0.7) the effects of Fermi motion become important, causing the effective quark distribution to extend far above x = 1, the kinematical limit being x = A. As a consequence also the gluon distribution in nuclei will differ from that in free nucleons as discussed in chapter 2. The best informations on the gluon and sea distributions have

been extracted up to now from neutrino-iron and neutrino-marble structure functions {7} and multimuon data from iron targets {22}. Therefore we have little information on the gluon distribution in a free nucleon so far, but its knowledge is essential for input to calculations for other processes like jet productions in $p\bar{p}$ collisions which are dominated by gluon-gluon interactions.

Probably there is little effect on the QCD analysis of data obtained with nuclear targets {23,24}. But one should keep in mind that the Altarelli-Parisi-equations require an integration from x to 1. In the case of nuclear targets the integral has to be extended to x=A, the x dependence of the structure functions, even if made QCD compatible, being unknown. Fortunately the contribution of this region to the integral is suppressed by the splitting functions, therefore it may not influence the result very much. But obviously a QCD analysis combining datasets of different nuclear targets should no longer be done.

Of course there is some impact on the interpretation as well of nucleon-nucleus scattering data, where in the analysis the same quark distributions for incoming and target nucleon are being used, as of $p\bar{p}$ which are usually compared to quark distributions obtained from nuclear targets instead to those from hydrogen targets.

But there is also an exciting consequence. For the first time nuclear effects have been observed on the quark level. This measurement of the change of quark distributions due to the nuclear surrounding may be the starting point for a lot of other investigations and open the door for the understanding of nuclear physics in terms of quarks and gluons.

4. THEORETICAL INTERPRETATIONS

At the time when the EMC data became known the effect appeared quite surprising and many people argued that one could hardly think of any mechanism which could produce the observed behaviour. They obviously did not realize that there have been many publications {25} and a lot of conferences like this one {26} where 'quarks (mesons) in nuclei' have been the main topic and where several phenomena have been discussed which indeed can change the quark distributions compared to the free nucleon case. But to my knowledge there existed only one publication by Krzywicki {27} which, although somehow hidden in the context, predicted, how one of those effects could influence the nucleon structure functions obtained in deep inelastic lepton nucleus scattering.

In the meantime a lot of theoretical papers has been published (and the number is still rapidly increasing) in which several phenomenological models are being used to

explain the effect. This audience has a lot of expertise concerning these models and we have heard several interesting presentations where they have been used for the description of other phenomena. Nevertheless let me (as an unexpert) try to summarize the main ideas and to put them into some order. For more details the reader is referred to the original references.

Before I start the discussion it is important to rise one basic question: is all effect due to iron or is it also caused by the deuterium? It is somehow funny that this question is not yet settled, although the deuteron is probably the nucleus which has been most extensively and carefully studied as well experimentally as theoretically. It is generally assumed that nuclear effects in the deuteron are small and well understood and that there are no other distortions to the quark distributions than those from Fermi motion effects. Experimental results indicate that this assumption is correct {28}. But recently there is again a lot of discussion going on and Frankfurt and Strikman {29} argue that nuclear effects inside the deuteron cause much larger corrections than the usual Fermi motion corrections {30,31}. Another example is the work by Glazek {32} which has been presented in a comment at this conference. He calculates that the assumption of the structure function being the sum of the structure functions for a free neutron and a free proton can be wrong on the 5-10% level already at low and medium x. At the moment this is still an open question and it might be that in the near future results concerning the ratio and the difference of neutron and proton structure functions extracted from deuterium data have to be revised.

Having this warning in mind let us turn to the existing theoretical explanations of the EMC effect which all assume that the observed effect is totally due to iron.

I have divided the models into different classes. Most of the model calculations can easily be sorted into one of them, but there are also a few which can not so easily be classified because they contain several ideas. If they are not as well presented as they would have served it, I apologize for this.

In the first approach part of the effect is explained by 'conventional nuclear physics'. It is based on the argument of Sullivan {33} that already the structure function for a free nucleon contains a contribution from the pion cloud associated with it: the virtual photon will either interact with a constituent of the nucleon or with a constituent of the surrounding pions. When several nucleons are brought together to form a nucleus there will be extra mesons associated with the exchange mechanisms responsible for the nuclear binding. It has been suggested by Llewellyn Smith {34} that these extra quasifree pions ($\sim$ 15% per nucleon) are responsible for the enhancement at low x. The measured structure function for iron contains an extra contribution which is a convolution of the probability $f_\pi(y)$ that a pion carries the

fraction y of the nucleon momentum and the pion structure function F_2^π. Ericson and Thomas {35} have shown (thick full curve in fig. 13) that magnitude and x dependence of the effect are well reproduced (for $x<0.3$) with this assumption and reasonable nuclear physics parameters. Llewellyn Smith in addition argued that the momentum taken by these extra quasifree pions should show up in a depletion of the nucleons valence quark distribution at high x as it is observed in the data. The authors also conclude that in nucleons with large neutron excess π^- production should be favoured over π^+ production. In their model the enhancement should grow approximately as the density of the nucleus and saturate for heavy nuclei. The mean numbers of excess pions and the associated contribution of Δ-states as calculated by Friman et al.{36} offer a good gideline.

The influence of extra pions in nuclei on the nucleon structure function has also been studied in detail by Berger et al. {37}. In their approach they use a pion density $f_\pi(y)$ and a pion structure function F_2^π which is quite different from the one used by Ericson and Thomas. They find that the magnitude of the effect at very small $x(\leq 0.1)$ cannot be explained in the context of known constraints to F_2^π unless they postulate an enhanced pion density of about 0.4 extra pions per nucleon which is roughly three times the value suggested by nuclear models. Even with this large number they are unable to fit the full x dependence of the measured ratio. They therefore conclude that other effects have to be present in addition which cause an intrinsic distortion of the nucleons in a nuclear medium.

What are these intrinsic distortions? The models available in the literature can be roughly divided into three different classes: in the first class the individual nucleon bags stay intact and don't change their quark content, but the internal properties like mass, radius or spin might be modified due to the presence of other nucleons; in the second class some of the nucleon bags loose their identity and form multiquark clusters and in the third class finally quarks are able to flow through the whole nucleus which then in an extreme view can be understood as one big bag.

Change of internal properties. There are two extreme models for a change of the nucleon radius r_N inside nucleons. An increase of r_N by about 30% compared to the free nucleon radius r_{free} has been proposed {38} to explain inelastic electron-^{56}Fe data {39}, the other model {40} demands that nucleons inside a nucleus should be compressed to bags of very small radii by a very significant pion cloud. There is some doubt on the accuracy of both calculations {41,42}. Nevertheless one should keep in mind that there is no evidence to suggest that the nucleon should not change its size when put inside a nucleus. Furthermore a collective change of the structure of each individual nucleon is probably the most easiest way to produce the large effect seen in the data. A small increase of r_N (which corresponds to an inversely

proportional decrease in mass) will reflect in a degradation of quark momenta to lower x.
Indeed Staszel et al. {43} get good agreement in the whole x range (dashed curve in fig. 11) with a decrease of effective nucleon mass (increase of nucleon radius) by about 13% and including Fermi motion corrections. Close et al. {44} conclude that an increase of confinement size of about 15% in iron compared to deuterium is needed to describe the data. I will come back to this model lateron in another context. Frankfurt and Strikman {29} argue that the observed behaviour is mainly a valence quark effect. In their model the increase at low x is due to antishadowing {45}, the relative enhancement at x around 0.1 for different nuclei should rise approximately like 1.8 log A. The behaviour at x>0.3 can be well explained by a swelling of nucleon size by only about 2.8% due to the nuclear surrounding. The predicted A-dependence of the effect at high x for mass numbers above around 12 is weaker than that at low x by about a factor of 2 while at lower mass numbers it is somewhat stronger. Also in another recent calculation by Levin and Ryskin {65} the EMC effect is explained by a swelling of nucleon size. To fit the experimental data they calculate an increase of the nucleon radius in iron of about 5.3 percent.

Although basically different the work of Fredriksson {46} somehow also fits into this class. In his model the nucleon is mostly in a bound quark-diquark state and the EMC effect is caused by an increase of radius of the dominating (ud) diquark in the nucleon surrounded by dense nuclear matter. This results in an change of Q^2-scale for two nuclei A_1 and A_2 by a multiplicative factor which is given by the ratio of the mean diquark radii squared for nuclei A_2 and A_1. Also Bjorken {47} interpretes the effect at high x as a change of the quark - diquark configuration due to the nuclear surrounding, without specifying in detail the mechanism for it.

A fraction of nucleons may transform into excited baryon states like Δ's. Szwed {48} claims that this fraction can be large in heavy nuclei. He calculates that a softening of the valence distribution can be explained if there is a 9-15% probability per nucleon of finding a Δ-isobar in a iron nucleus (dashed-dotted curve in fig. 11: 15% Δ-admixture; full curve: 9% admixture plus 3.3% decrease in gluonmomentum). With this fraction the data are well reproduced,but it seems unreasonably high compared to measurements and theoretical calculations {36,49}.

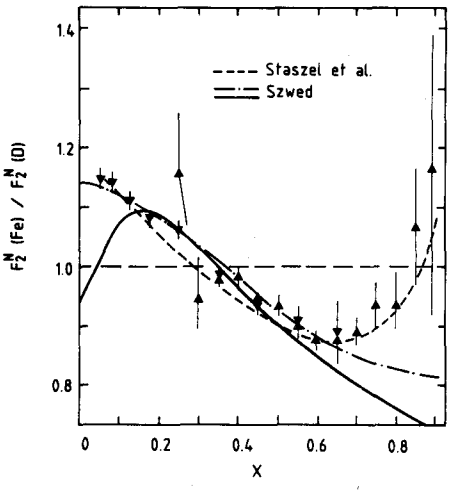

Fig. 11. Model calculations for the EMC effect-change of internal nucleon properties

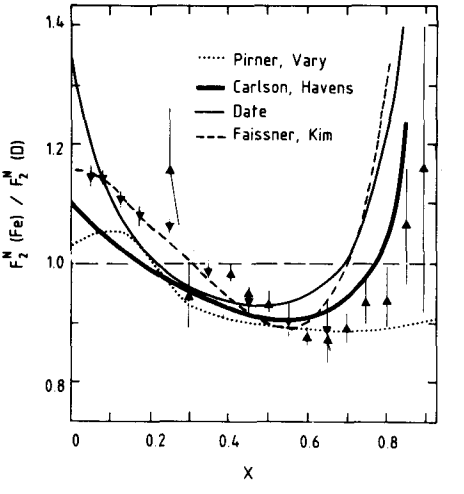

Fig. 12. Model calculations for the EMC effect-multiquark states

Multiquark states. In the second class of models the quarks are no longer confined in their original nucleon bags but there is a certain probability that these bags can overlap and multiquark states are formed which contain six valence quarks ($|6q\rangle$), nine valence quarks ($|9q\rangle$), etc. This might be not so unlikely even at normal densities, for the mean nucleon distance in a high A nucleus is around 1.8 fermi compared to the free nucleon bag radius of around 1 fermi in the MIT bag model. Jaffee {50} was the first one to react on the experimental data and his paper contains several ideas which then have been picked up by other authors. He supposes that two nucleons may coalesce in $|6q\rangle$ bags, having a bigger radius than $|3q\rangle$ bags, the longer range being responsible for an enhancement of the quark distributions at low x. He calculates an increase of the sea in iron compared to deuterium of 60% and a softening as well of the valence as the gluon distribution. In figure 12 the results of several other calculations using this concept of multiquark states are shown. Pirner and Vary {51} (dotted curve) use a 16% probability for a nucleon being in a $|6q\rangle$ cluster, the same number they have evaluated to fit inelastic ^{3}He data {52}. Carlson and Havens {53} (thick full curve) choose a fraction of 30% of nucleons to become part of $|6q\rangle$ clusters which from counting rule arguments have much steeper x distributions for valence and sea quarks than for free nucleons. Date {54} (thin full curve) also includes clusters with more than

six valence quarks. He finds that sea quarks in multiquark states have to be enhanced while the gluons are rather suppressed compared to the free nucleon case. Faissner and Kim {55} use a very special class of multiquark clusters. They started from the observation that α-clusters play a dominant role in many nuclei. They assume that these α-clusters are bags of 12 valence quarks, the 6u and 6d quarks, forming a singlet in spin, isospin and colour, moving freely in it. This assumption, however, is in contradiction to other multiquark state calculations which predict only a very small fraction of 12-quark states in ^{4}He {56}. Including Fermi motion correction without high momentum tail for the nucleons and having an effective quark mass as additional parameter they get good agreement (dashed curve) with the data if (20 ± 5)% of the nucleons are contained in these $|12q>$ clusters. They predict a very strong effect for ^{4}He and also for ^{12}C, ^{16}O and similar nuclei, but apart from this a roughly constant EMC effect throughout the periodic table, for the fraction of α clusters in normal nuclei is roughly constant.
Also another interpretation of the EMC effect by Cohen-Tannoudji and Navelet {57} is based on the idea of multinucleon clusters together with ingredients from QCD.

Quark percolation - the nucleus as one big bag. The last class of models goes even one step further and treats the nucleus as one big bag. If the baryon density inside a nucleus becomes big enough many nucleon bags may overlap in such a way that finally quarks will be able to move freely through the whole nucleus. This free flow of quarks (colour) is known as percolation {58}. In the extreme view the nucleus then can be treated no longer as an assembly of n nucleons or some nucleons plus multiquark bags but as one single bag inside which the 3n valence quarks and the sea quarks are completely delocalized. Calculations using this approach in another context have been performed by Bleuler et al. {59} and presented to this conference by Petry {60}. They show that characteristic nuclear properties connected with conventional shell structure are obtained in a natural way by starting directly from this enlarged scheme.
In the model of Nachtmann and Pirner {61} the quarks can extend over the whole transverse size of the nucleus with radius R_A. They conclude that in this case no longer Q^2 is the relevant parameter but $Q^2 . R_A^2$. This means that for fixed x the structure function for deuterium measured at $Q'^2 = Q^2 . (R_{Fe}^2/R_D^2)$ should be the same as for iron at Q^2. Thus the observed difference of Fe and D is purely a scale change similar to the model of Fredriksson {46} and of Close et al. {44} mentioned above where it is caused by the increase of diquark or of nucleon size, respectively. The latter authors have empirically determined a Q^2 scale factor of around 2 while Nachtmann and Pirner get a factor of $R^2_{Fe}/R^2_D = 4.5$ which is clearly an overestimation of the effect. It follows automatically from these models that the difference of the structurefunction for all nuclei should disappear at the same x as the scaling violations do. In the Nachtmann-Pirner approach the deviation from unity for the ratio of the structurefunction for two different nuclei A_1 and A_2 at fixed x should in

first order be directly proportional to ln $(R_{A_1}^2/R_{A_2}^2)$ times the slope of ln $F_2(x,Q^2)$ versus ln Q^2 at this value of x. In my opinion the deuteron nucleus is too untypical to fit really in this 'big bag' picture and data from other nuclei (when being available) should be used to test the validity of this model. The picture of the nucleus as one big bag is also the basis of the work of Krzywicki {27}. He argued that in a snapshot of a nucleus one could not distinguish between virtual particles emitted and eventually reabsorbed by the same nucleon and those exchanged between different nucleons. He therefore treated the nucleus as one single bag of partons. The clue of his model is that this single bag contains an additional amount of sea quarks which then is responsible for the change of the nucleon structure function A paper by Furmanski and Krzywicki {62} extends this work (dashed-dotted -curve in fig. 13). In their model the effect saturates for A>20, while in a similar approach by Godbole and Sarma {63} (thin full curve in fig. 13) it rises approximately with mass number A.

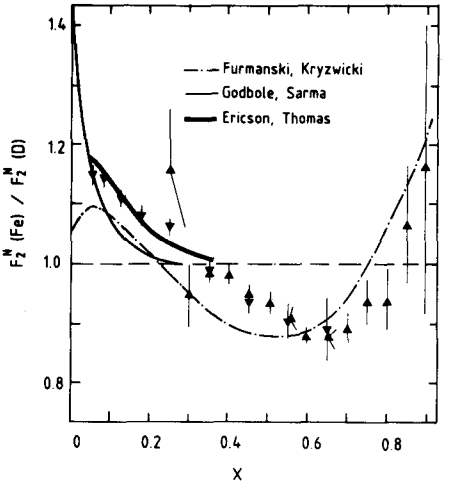

Fig. 13. Model calculations for the EMC effect-sea enhancement.

Finally there is another interesting paper by Barshay {64}. He predicts a strong effect in the tightly bound systems of He^3 and He^4 which is due to extra gluons and their self coupling. A part of the momentum is taken from the valence quarks to

these extra gluons and a fraction of it again reappears in the sea quark distribution. The effect on medium-weight and heavy nuclei then would originate from the heliumlike clusters in these systems as it is proposed by Faissner and Kim {55}.

5. CONCLUSION

Deep inelastic scattering experiments with charged leptons have shown that the quark and gluon distributions in nuclei are different from those in free nucleons. The global features of the observed effect can be described by many 'simple' models but obviously more experimental information is needed to decide definitely which explanation is correct. As a first step a measurement of the A dependence has already been performed at low Q^2 in a SLAC experiment {66}. This has taken data with several targets ranging from deuterium and helium to gold. Preliminary results indicate a mild increase of the effect at high x with A up to the highest mass numbers, final results are expected shortly. A low angle experiment will be performed this autumn by the EMC to study for several nuclei the region at low x and low Q^2 where shadowing and nuclear effects seem to counteract each other. Measurements on several targets at higher Q^2 will be done by the two muon experiments EMC and BCDMS at CERN and data from different targets are also being compared by several neutrino experiments {67}. The EMC has already performed some studies of hadronic final states from nuclear targets and intends to continue this investigations with an upgraded apparatus. This group also tries to get out more information on the gluon distribution in different nuclei by comparing J/ψ events from hydrogen, deuterium and iron.

So there is a lot of experimental and theoretical work going on and all of this will hopefully help to develop a common understanding of nuclear and particle physics in terms of quarks and gluons.

REFERENCES

1. EMC, J.J. Aubert et al., Phys. Lett. 123B (1983) 275.
2. BCDMS, A. Argento et al., Phys. Lett. 120B (1982) 245.
3. For details see: F.E. Close, An Introduction to Quarks and Partons, Academic Press 1979.
4. S.D. Drell, T.M. Yan, Ann. Phys. (N.Y.) 66, (1971) 578.
5. EMC, J.J. Aubert et al., Phys. Lett. 121B (1983) 87.
6. A. Bodek et al., Phys. Rev. D20 (1979) 1471.
7. See for instance: CDHS, H. Abramowicz et al., Z. Phys. C 17 (1983) 283; CHARM, F. Bergsma et al., Phys. Lett. 123B (1983) 269.
8. G. Altarelli and G. Parisi, Nucl. Phys. B126 (1977) 298.
9. For a review see for instance: J. Drees, Proceedings of the 1981 Int. Symposium and Lepton and Photon Interactions at High Energies, ed. W. Pfeil, Bonn 1981, P. 474; F. Eisele, Proceedings of the 21st Int. Conference on High Energy Physics, ed. P. Petian and M. Porneuf, Paris 1982, P. C3-337.

10. EMC, J.J. Aubert et al., Phys. Lett. 105B (1981) 315.
11. EMC, J.J. Aubert et al., Phys. Lett. 123B (1983) 123.
12. EMC, J.J. Aubert et al., Phys. Lett. 105B (1981) 322.
13. EMC, J.J. Aubert et al., Nucl. Inst. Meth. 179 (1981) 445.
14. A. Bodek and J.L. Ritchie, Phys. Rev. D23 (1981) 1070; D24 (1981) 1400.
15. See ref. 14 and L.L. Frankfurt and M.I. Strikman, Nucl. Phys. B181 (1981) 22.
G. Berlad et al., Phys. Rev. D22 (1980) 1547.
16. K. Rith, preprint Freiburg university THEP 83/4 (1983) (to appear in the Proceedings of the XVIII Rencontre de Moriond 1983).
17. A. Bodek et al., Phys. Rev. Lett. 30 (1973) 1087; A. Bodek et al., Phys. Lett. 51B (1983) 417; A. Bodek et al., Phys. Rev. D20 (1979) 1471.
18. A. Bodek et al., Phys. Rev. Lett. 50 (1983) 1431.
19. A. Bodek et al., Phys. Rev. Lett. 51 (1983) 534.
20. S. Stein et al., Phys. Rev. D12 (1975) 1884.
21. D.O. Caldwell et al., Phys. Rev. Lett. 42 (1979) 553; Phys. Rev. D7 (1973) 1362; A.M. Eisner in "Proceedings of the 1979 International Symposium on Lepton and Photon Interactions, Fermilab, Aug. 1979, p. 448; T.B.W. Kirk and H.D.I. Abarbanel ed.
22. EMC, J.J. Aubert et al., Nucl. Phys. B213 (1983) 1; BFP, A.R. Clark et al., Phys. Rev. Lett. 45 (1980) 682.
23. C.H. Llewellyn Smith, Phys. Lett. 128B (1983) 107.
24. C.H. Llewellyn Smith, Oxford University preprint 37/83 (1983).
25. For references see for instance: A.W. Thomas, CERN-TH 3368 (1982) (to appear in Advances in Nuclear Physics, Vol. 13 (1983).
26. See for instance: Nucl. Phys. A335 (1980); Nucl. Phys. A358 (1981); Nucl. Phys. A374 (1982); Progress in nuclear and particle physics, ed. D. Wilkinson, Vol 1 (1978), Vol 8 (1982); 'Mesons in nuclei', ed. M. Rho and D. Wilkinson, North Holl. 1979.
27. A. Krzywicki, Phys. Rev. D14 (1976) 132.
28. A. Bodek, University of Rochester, preprint UR 858, COO-3065-365 (1983) to appear in the Proceedings of the XIV International Multi Particle Symposium, Lake Tanoe, 1983.
29. L.L. Frankfurt and M.I. Strikman, Leningrad preprint 886 (1983).
30. G. West, Phys. Lett. 18 (1971) 509.
31. W.B. Atwood and G.B. West, Phys. Rev. D7 (1973) 773; L.L. Frankfurt and M.I. Strikman, Nucl. Phys. B148 (1979) 107.
32. S. Glazek, University of Warsaw Preprint 1983 and contribution to the International Europhysics conference of High Energy Physics, Brighton (UK), 1983, paper 27.
33. J.D. Sullivan, Phys. Rev. D5 (1972) 1732.
34. C.H. Llewellyn Smith, Phys. Lett. 128B (1983) 107.
35. M. Ericson and A.W. Thomas, Phys. Lett. 128B (1983) 112.
36. B.L. Friman et al., Phys. Rev. Lett. 51 (1983) 763.
37. E.L. Berger et al., Argonne preprint ANL-HEP-PR-83-24 (1983).
38. J.V. Noble, Phys. Rev. Lett. 46 (1981) 412.
39. R. Altemus et al., Phys. Rev. Lett. 44 (1980) 965.
40. G.E. Brown and M. Rho, Phys. Lett. 82B (1979) 177; G.E. Brown et al., Phys. Lett. 94B (1979) 383.
41. P.D. Zimmermann, Phys. Rev. C26 (1982) 265.
42. G.A. Miller, CERN TH-3516 (1983).
43. M. Staszel et al., University of Warsaw preprint IFT/9/83 (1983).
44. F.E. Close et al., Phys. Lett. 129B (83) 346.
45. N.N. Nikolaev and Z.I. Zakharov, Phys. Lett. 55B (1975) 397.
46. S. Fredriksson, Stockholm preprint TRITA-TFY-83-15 (1983).
47. J.D. Bjorken, unpublished note.
48. J. Szwed, Phys. Lett. 128B (1983) 245.
49. V. Bakken et al., Physica Scripta 19 (1979) 491; L.L. Frankfurt and M.I. Strikman, Phys. Rep. 76C (1981) 215.
M. Harvey, Nucl. Phys. A352 (1981) 326; M.H. Storm and A. Watt, Nucl. Phys. A to be published.
50. R.L. Jaffe, Phys. Lett. 50 (1983) 228.
51. M.J. Pirner and J.P. Vary, University of Heidelberg preprint UNI-HD-83-02 (1983)

52. H.J. Pirner and J.P. Vary, Phys. Rev. Lett. 46 (1981) 1376.
53. C.E. Carlson and T.J. Havens, Phys. Rev. Lett. 51 (1983) 281.
54. S. Date, Waseda University preprint WU-HEP-83-4 (1983) (submitted to Phys. Rev Lett.).
55. H. Faissner and B.R. Kim, Phys. Lett. 130B (1983) 321.
56. M. Namiki et al., Phys. Rev. C25 (1982) 2157.
57. G. Cohen-Tannoudji and H. Navalet, Saclay preprint SPhT-83-97 (1983).
58. G. Baym, Physica 96A (1979) 131.
59. K. Bleuler et al., University of Bonn Preprint (1983).
60. H.R. Petry, these proceedings.
61. O. Nachtmann and H.J. Pirner, University of Heidelberg preprint HD-THEP-83-8 (1983).
62. W. Furmanski and A. Krzywicki, Orsay preprint LPTHE 83/11 (1983).
63. R.M. Godbole and K.V.L. Sarma, Phys. Rev. D25 (1982) 120, and private communication.
64. S. Barshay, TH. Aachen preprint (1983).
65. E.M. Levin and M.G. Ryskin, Leningrad preprint 888 (1983).
66. R.G. Arnold et al., SLAC experiment E139.
67. For a compilation of these results see:
K. Rith, Freiburg preprint THEP 83/5, to appear in the proceedings of the International Europhysics Conference on High Energy Physics, Brighton (UK), (1983).